This is a non-peer reviewed preprint submitted to EarthArXiv.

This preprint was also submitted to Groundwater for peer review.

Temporal convolutional networks for subsidence prediction in snowy regions

Satoshi Tajima[1, 2, 3]

[1] Centre for Hydrogeology and Geothermics, University of Neuchâtel, Neuchâtel, Switzerland

[2] Climate and Environmental Physics, University of Bern, Bern, Switzerland

[3] Graduate School of Frontier Sciences, The University of Tokyo, Kashiwa, Japan

Correspondence to: satoshi.tajima@unine.ch

Key words

Temporal convolutional network (TCN), Land subsidence, Snow-melting system, Machine learning, Sequential modelling, Real-time prediction

Article Impact Statement

Temporal convolutional networks (TCNs) can effectively predict land subsidence caused by groundwater abstraction for snow melting.

Abstract

This paper introduces a model based on a temporal convolutional network (TCN) for predicting future land subsidence caused by groundwater pumping for snow melting. Developed using historical snowfall and cumulative subsidence data from Joetsu City, Japan, the model demonstrates satisfactory performance in predicting observed land subsidence. The results suggest that TCNs are effective for real-time predictions of land subsidence associated with snow melting, thanks to their efficient computational capabilities, broad applicability to practical problems, and minimal data requirements. The proposed approach facilitates responsive and effective land subsidence prevention through proactive pumping management in regions with heavy snowfall.

1 . Introduction

Land subsidence is the gradual or sudden downward movement of the Earth's surface (Galloway and Burbey 2011, Ma et al. 2018, Bagheri-Gavkosh et al. 2021), which can lead to irreversible environmental impacts (Gambolati 1975, Holzer and Galloway 2005). Land subsidence can occur due to natural factors such as tectonic activity, sediment compaction, and permafrost degradation (e.g. Barends et al. 1995, Xu et al. 2008, Modoni et al. 2013, Liu et al. 2023, Shirzaei et al. 2021), yet these natural causes account for only 23% of global occurrence of land subsidence (Bagheri-Gavkosh et al. 2021). The remaining 77% are attributed to human activities (Bagheri-Gavkosh et al. 2021), with groundwater extraction being a primary driver (Galloway and Burbey 2011, Bagheri-Gavkosh et al. 2021, Shirzaei et al. 2021, Gambolati and Teatini 2015). When groundwater is extracted, the decrease in pore pressure increases the effective stress on the subsurface, leading to the compaction of aquifer systems and subsequent land subsidence (Galloway and Burbey 2011, Bagheri-Gavkosh et al. 2021, Shirzaei et al. 2021, Gambolati and Teatini 2015). In regions with significant snowfall, groundwater is frequently used in snow-melting systems that sprinkle groundwater onto road surfaces to clear snow and ice (Kayane 1980, Sekiya and Tohno 1997, Morita and Tago 2005). The relatively stable year-round temperature of groundwater makes it an ideal resource for this purpose. However, the excessive abstraction of groundwater for snow melting can exacerbate land subsidence (Kayane 1980, Sekiya and Tohno 1997, Morita and Tago 2005), and thus the prediction of land subsidence is crucial for its prevention through effective pumping management.

Conventional methods for predicting land subsidence primarily rely on numerical simulations, which model the physical behaviour of solid materials (Shirzaei et al. 2021), using pumping rates as inputs (e.g. Gambolati and Freeze 1973, Zhang et al. 2012, Ortega-Guerrero et al. 1999). Although numerical simulations are powerful, they require detailed field data on subsurface properties material such as hydraulic conductivity and bulk modulus. In practice, however, such in-situ data are often unavailable. Even if available, they are usually accompanied by uncertainties and demand scrupulous model calibration (Aichi 2020, Smith and Knight 2019, Gambolati 1975), thereby complicating real-time predictions. Moreover, especially in predicting subsidence resulting from groundwater abstraction for snow melting, physics-based simulations may encounter challenges in accurately incorporating pumping estimates derived from snowfall data.

An alternative method is the data-driven approach. Mizumura (1994) implemented this method to predict temporal land subsidence using historical data on subsidence, water table elevation, and snowfall through Kalman filtering. This approach bypasses the need for detailed data on subsurface material properties and can integrate snowfall data, making it advantageous over numerical simulations for practical applications. However, the Kalman filtering used by

Mizumura (1994) assumes Gaussian noise and linear correlations among variables, which may limit its effectiveness in real-world applications where noise characteristics contain complexity, and system dynamics are often nonlinear.

To overcome these limitations, this study proposes the use of temporal convolutional networks (TCNs) (Bai et al. 2018) (see Section 2 for details), a machine learning approach that can model nonlinear relationships without assuming specific noise structures. TCNs have been successfully applied to various sequence modeling tasks in hydrology, including predictions of water quality parameters (Zhang and Li 2023), groundwater level (Zhang et al. 2023, Haider et al. 2023), and mine water inflow rate (Yang et al. 2023). Recent studies have demonstrated TCNs' superior predictive accuracy compared to other models, such as recurrent neural networks (RNNs) and long short-term memory (LSTM) networks (e.g. Chen et al. 2020, Bai et al. 2018, Wan et al. 2019, Lara-Benítez et al. 2020). Furthermore, TCNs offer faster computational speeds in both training and evaluation due to their ability to process temporal data in parallel (Bai et al. 2018).

This paper proposes a TCN model to predict future land subsidence based on historical data on snowfall and cumulative subsidence. Using data from Joetsu City in northwestern Japan, where intensive groundwater abstraction for snow melting has led to notable subsidence, the TCN model is optimized through hyperparameter tuning, and its performance is evaluated.

2. Temporal Convolutional Networks (TCNs)

Before introducing the concepts of TCNs, this section first defines the general sequential modeling task. Given an input sequence $\mathbf{x} = x_0, x_1, \dots, x_T$ and corresponding observation data for outputs $\mathbf{y} = y_0, y_1, \dots, y_T$, where the subscripts represent time steps, the goal is to generate predictions $\hat{\mathbf{y}} = \hat{y}_0, \hat{y}_1, \dots, \hat{y}_T$. This involves finding a function $\mathcal{G}: \boldsymbol{x} \rightarrow \hat{\boldsymbol{y}}$ that minimizes the loss between the observations and predictions, $\mathcal{L}(y, \hat{\boldsymbol{y}})$.

A TCN is characterized by causal dilated convolutions (Figure 1a). The term causal refers to the convolution property where the output at a specific time, $\hat{y}_t$, is influenced only by the current and past data points, $x_0, x_1, \dots, x_t$. This means that there is no information leakage from future time steps to past (Bai et al. 2018). Furthermore, dilated convolutions are employed to capture long-term information by enabling a large receptive field (Bai et al. 2018, Yu and Koltun 2015). The dilated convolution $\mathcal{D}$ for an element τ in a sequential layer λ is expressed as

$$\mathcal{D}(\lambda, \tau) = (x * \mathcal{F})(\lambda, \tau) = \sum_{i=0}^{k-1} \mathcal{F}(i) x^{\lambda}_{\tau - d_\lambda i}, \quad (1)$$

where $*$ denotes the convolution operation, $\mathcal{F}: \{0, 1, \dots, k-1\} \rightarrow \mathbb{R}$ represents the filter (Bai et al. 2018), and **d** is the vector of dilations for each residual block (Remy 2020). The receptive field (R) is calculated as

$$R = 1 + 2(k-1)N_s \sum_j d_j \,, \tag{2}$$

where k is the kernel size, N_s is the number of residual block stacks (Figure 1b). To produce outputs with the same length as that of input, zero padding of a length $k - 1$ is added to each layer except for the final output layer (Bai et al. 2018).

TCNs contain residual blocks (He et al. 2016) to facilitate learning, particularly in deep networks (Figure 1b). Each residual block consists of two layers of causal dilated convolutions. Weight normalization (Salimans and Kingma 2016) is applied to each convolution before passing through an activation function, which in this study is the rectified linear unit (ReLU) (Nair and Hinton 2010). A spatial dropout (Srivastava et al. 2014) is applied following each activation function.

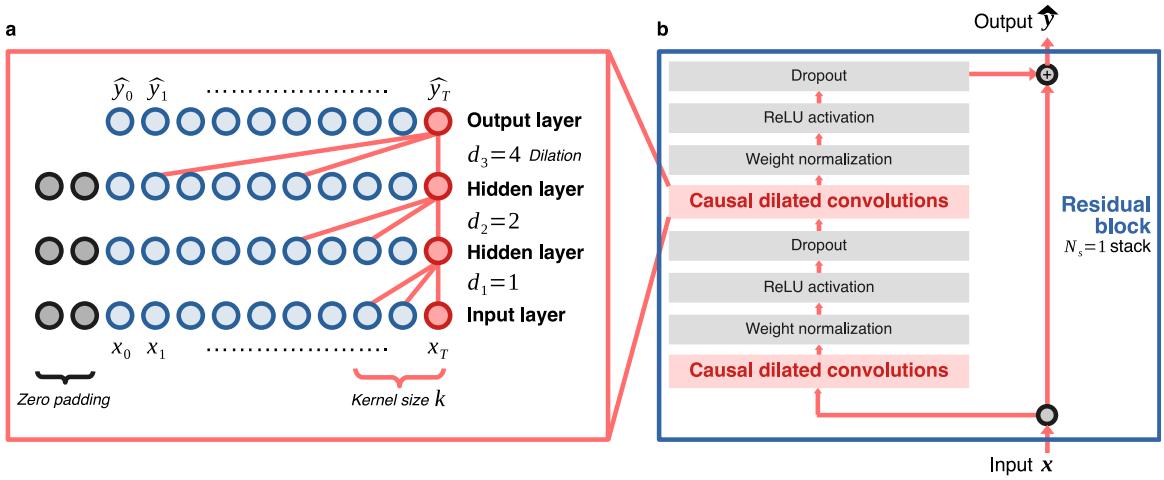

Figure 1. Schematics of **a** causal dilated convolution and **b** residual block in TCN.

3. Method

3.1. Study area

The study area is Joetsu City in Niigata Prefecture, Japan (Figure 2), known for its heavy winter snowfall. The average annual cumulative snowfall in Joetsu is 413 cm, with a recorded maximum snow depth of 96 cm (Japan Meteorological Agency 2021).

To manage this snow, groundwater is abstracted for use in snow-melting systems. This practice was initially introduced in Joetsu following its first practical application in Nagaoka, another city in the same prefecture. However, in the late 1970s, Joetsu City began to experience declines in groundwater levels and associated land subsidence due to groundwater extraction for snow melting (Sekiya and Tohno 1997). Notably, in 1984, during a period of heavy snowfall, the city recorded an annual subsidence rate of 10.1 cm, the highest in Japan at that time

(Environmental Agency of Japan 1985). In response, national and local authorities developed the Basic Guidelines for Land Subsidence Prevention in the Joetsu Region in 1987. These guidelines include measures such as requiring notification for the installation of new wells and regular monitoring of groundwater levels and land subsidence. Alerts and warnings are issued if these values fall below prescribed standards.

The urban area of Joetsu City is situated in the Takada Plain. The majority of the plain is composed of Quarternary sediments, with an average layer thickness of approximately 300 m. A clay layer of 40–60 m in thickness (Sekiya and Tohno 1997) is present at the top, underlain by a gravel aquifer with a thickness of 8–14 m (Tohno and Sekiya 1997). Subsequently, clay and gravel layers emerge alternately (Tohno and Sekiya 1997). Groundwater is extracted from multiple gravel aquifers, inducing the compaction of the upper clay layers and resulting in the land subsidence.

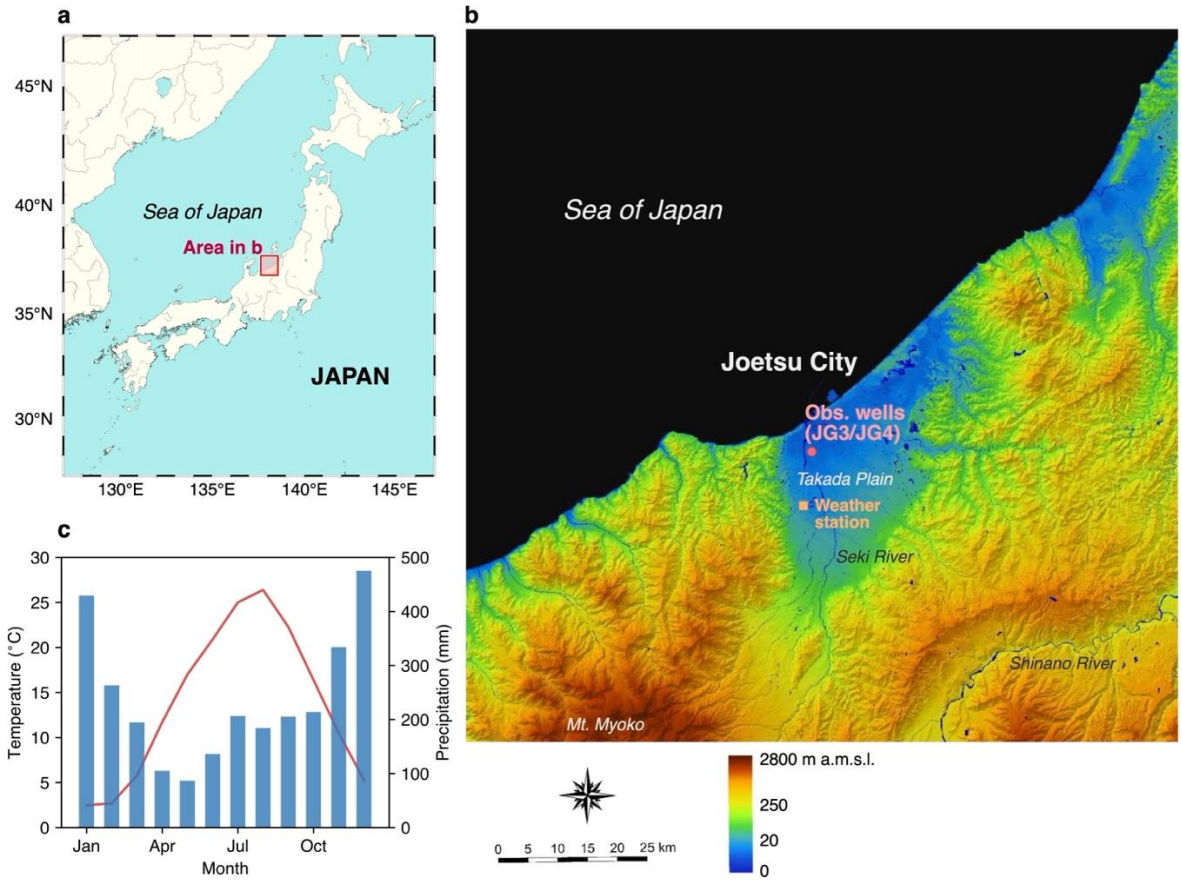

Figure 2. a Wide-area map, **b** topographical map (modified from Geospatial Information Authority of Japan (2019)), and **c** climograph (data from Japan Meteorological Agency (2021)) of study area.

3.2. Data acquisition and preprocessing

The TCN model utilizes temporal data on snow accumulation from the Takada weather station

(Japan Meteorological Agency 2024) (Figure 2b) and cumulative land subsidence measurements from December 2015 to July 2024 (Figure 3). The land subsidence data have been continuously recorded by Niigata Prefecture at two observation wells, “Joetsu-G3 (JG3)” and “Joetsu-G4 (JG4)” (Figure 2b). Both datasets have a temporal resolution of 1 hour. The input features for the TCN prediction include temporal data on snow accumulation combined with historical cumulative land subsidence data, which serves as the target feature.

For preprocessing, the datasets were divided into training (80%) and testing (20%) subsets. To enhance the prediction accuracy of the TCN, the input data were standardized using the following formula:

$$x_i' = \frac{x_i - \mu}{\sigma}, \tag{3}$$

where x_i' denotes the standardized data at time i, x is the original data, and μ and σ represent the mean and standard deviation of the training data, respectively. Note that even for scaling the testing data, the statistical parameters for the training data are used.

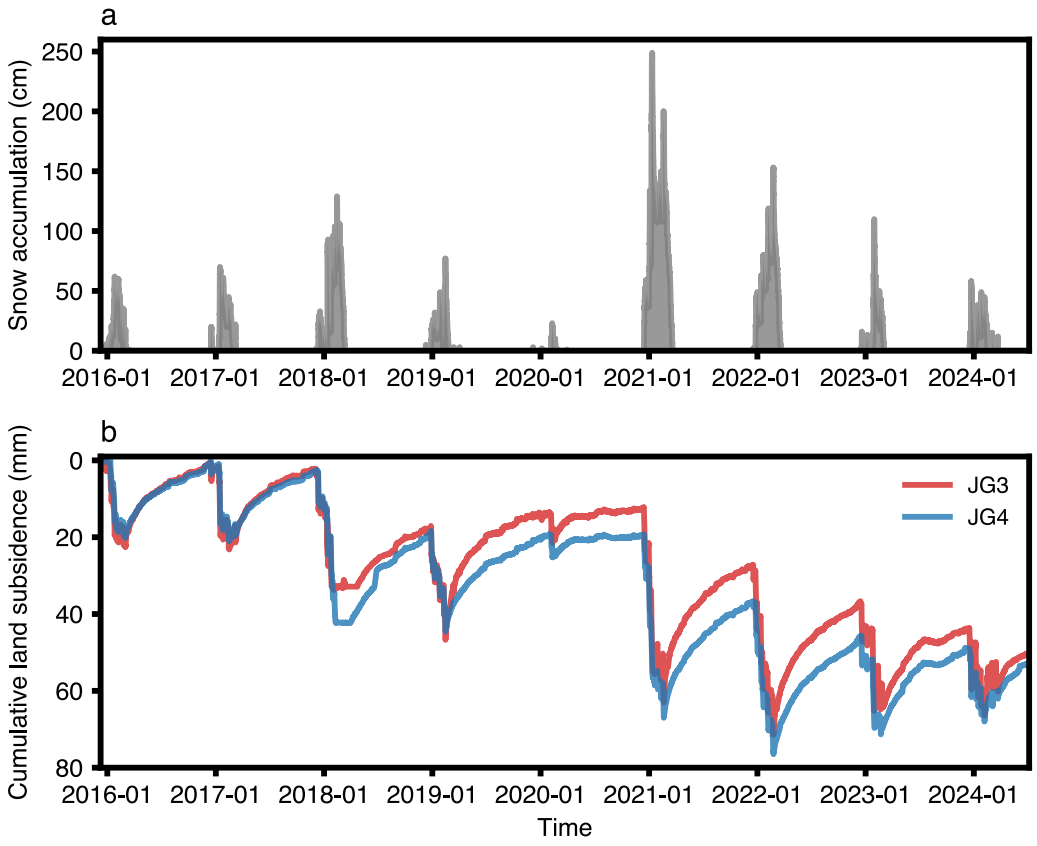

Figure 3. Temporal data of **a** snow accumulation at Takada (Japan Meteorological Agency 2024) and **b** cumulative land subsidence of observation wells JG3 and JG4.

3.3. TCN implementation

The Adam optimizer (Kingma and Ba 2014) is used for training the TCN model, and the mean absolute error (MAE) (Equation 4) as the loss function. The initial learning rate is set to 10^{-3}, which is reduced by a factor of 5, with a lower bound of 10^{-5}, if the loss function ceases to improve. The training is conducted over a maximum of 100 epochs, with early stopping applied to mitigate overfitting (Raskutti et al. 2014). The TCN network architecture includes a single causal convolutional layer (N_s = 1) with dilutions **d** = [1, 2, 4].

To identify the optimal hyperparameters, various kernel sizes k = 3, 4, 5 and batch sizes N_b = 4, 8, 16 were tested and compared (Table 1). For this comparison, the TCN training is performed for 100 epochs with early stopping disabled. In all tested cases, the condition $N_b > R$ (Equation 2) is satisfied.

TCN training and predictions were conducted 10 times for each well and for each combination of k and N_b, with results averaged for analysis.

Table 1. Performance of TCN prediction for observation well JG3 with various hyperparameter sets. Optimal set is shown by bold. TCN training is performed for 100 epochs.

Kernel size (k)	**Batch size (N_b)**	**MAE (mm)**	$\boldsymbol{R^2}$
3	4	0.150	0.999
3	8	0.186	0.997
3	16	0.458	0.989
4	**4**	**0.140**	**0.999**
4	8	0.247	0.997
4	16	0.440	0.990
5	4	0.193	0.998
5	8	0.218	0.997
5	16	0.379	0.992

3.4. Model performance evaluation

The model performance is evaluated using MAE and the coefficient of determination (R^2). These metrics are defined as

$$MAE = \frac{1}{N}\sum_{i=1}^{N}|\hat{y}_i - y_i| \tag{4}$$

$$R^2 = 1 - \frac{\sum_{i=1}^{N}(y_i - \hat{y}_i)^2}{\sum_{i=1}^{N}(y_i - \bar{y})^2}, \tag{5}$$

where N represents the total number of data points, y_i and $\hat{y}_i$ denote the observed and predicted values of the target variable, cumulative land subsidence, at time i, respectively, and y is the mean

of the observed values. These metrics satisfy $MAE \geq 0$ and $0 \leq R^2 \leq 1$. The MAE quantifies the average absolute deviation of predictions from the observed values, with smaller values indicating better model performance. The R^2 value measures the proportion of the variance in the observed data that is predictable from the model, where a value closer to 1 signifies an accurate model prediction.

4. Results and discussion

The optimal hyperparameters for the TCN prediction are k = 4 and N_b = 4 (Table 1). With these hyperparameter values, the MAE is 0.140 mm, which corresponds to approximately 0.2% of the maximum observed cumulative land subsidence. The following discusses the TCN prediction results based on the optimal hyperparameter selection.

Figure 4 demonstrates that the TCN predictions fit well to the observed cumulative land subsidence at the observation wells JG3 and JG4. The MAE values are 0.154 and 0.285 mm, and R^2 = 0.999 and 0.997 for JG3 and JG4, respectively. As early stopping is implemented, the TCN training was terminated after 57 and 60 epochs for JG3 and JG4, respectively, prior to the permitted limit of 100 epochs. The TCN model effectively captures the short-term fluctuations in the observed land subsidence during winter, which are induced by groundwater abstraction for snow-melting systems. Furthermore, the TCN accurately represents the long-term trend, including seasons without snowfall, which reflects the recovery from intensive winter subsidence.

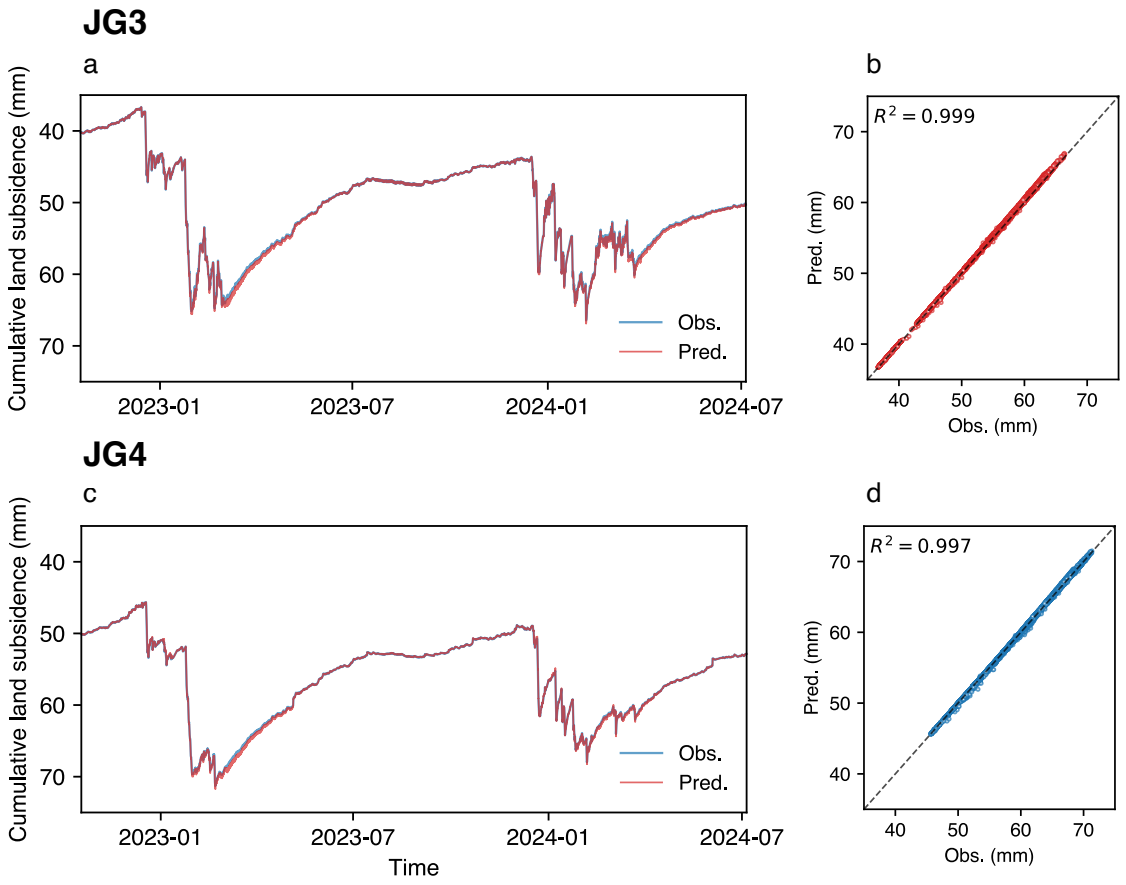

Figure 4. a, c Time-series and **b, d** correlation plots for observed cumulative land subsidence and TCN predictions with optimal hyperparameter sets (k = 4, N_b = 4) for each observation well. Early stopping is implemented.

The results suggest that TCNs are advantageous for the real-time prediction of the land subsidence induced by groundwater abstraction for snow melting from three perspectives:

- **Efficient computation.** TCNs require relatively limited computational time. In this study, a single TCN run, including both training and prediction, had an average processing time of approximately 30 seconds. The prediction component itself required less than a second.
- **Broad practical applicability.** Unlike classical Kalman filters, which rely on the assumption of linear correlations among variables with Gaussian noise (Mizumura 1994), TCNs can handle nonlinear dynamics without such assumptions, thus being suitable for a wider range of complex real-world problems.
- **Minimal data requirements.** Unlike numerical simulations, TCNs does not require detailed field data on subsurface material properties, making them particularly valuable in regions with limited field data availability. Moreover, TCNs do not require temporal data on water table elevation or pumping rates as inputs. Once trained on historical data of snow accumulation and

land subsidence, TCNs can predict future land subsidence using only snowfall forecast data. Short-term predictions of snow accumulation can be obtained from weather forecasts, whereas similar predictions for water table elevation and pumping rates are generally unavailable. Overall, TCNs facilitate the real-time prediction of land subsidence associated with snow melting, thereby enabling proactive pumping management. By implementing real-time predictions, subsidence alerts can be issued before intensive groundwater abstraction and the subsequent occurrence of land subsidence when heavy snowfall is anticipated. Thus, TCNs contribute to the responsive and effective prevention of land subsidence in regions prone to heavy snowfall.

TCNs require comprehensive long-term historical data for effective training, which is often unavailable in real fields. Therefore, continuous monitoring of snow accumulation and land subsidence is crucial for the successful practical implementation of the TCN for predicting land subsidence induced by groundwater abstraction for snow melting.

5. Conclusion

This paper presents a model based on a temporal convolutional network (TCN) for predicting future land subsidence due to groundwater abstraction for snow melting. The results demonstrate satisfactory performance in predicting observed land subsidence. This finding indicate that TCNs facilitate real-time predictions of land subsidence associated with snow melting, thereby enabling responsive and effective land subsidence prevention through proactive pumping management in regions prone to heavy snowfall.

Acknowledgments

The author is grateful to the Joetsu City Office for providing the temporal data of observed cumulative land subsidence. The author declares no conflict of interest.

References

Aichi, M. 2020. Land subsidence modelling for decision making on groundwater abstraction under emergency situation. *Proceedings of the International Association of Hydrological Sciences* 382: 403–8.

Bagheri-Gavkosh, M., S. M. Hosseini, B. Ataie-Ashtiani, Y. Sohani, H. Ebrahimian, F. Morovat, and S. Ashrafi. 2021. Land subsidence: A global challenge. *Science of The Total Environment* 778: 146193.

Bai, S., J. Z. Kolter, and V. Koltun. 2018. An empirical evaluation of generic convolutional and recurrent networks for sequence modeling. *arXiv preprint arXiv:1803.01271*.

Barends, F. B., F. J. Brouwer, and F. H. Schröder. 1995. *Land subsidence*. IAHS.

Baù, D. 2022. Land subsidence surrogate models for normally consolidated sedimentary basins. *Geomechanics for Energy and the Environment* 32: 100297.

Chen, Y., Y. Kang, Y. Chen, and Z. Wang. 2020. Probabilistic forecasting with temporal convolutional neural network. *Neurocomputing* 399: 491–501.

Environmental Agency of Japan. 1985. Overview of land subsidence areas in Japan.

Frigo, M., M. Ferronato, L. Gazzola, P. Teatini, C. Zoccarato, M. Antonelli, A. Corradi, M. C. Dacome, M. D. Simoni, and S. Mantica. 2020. Numerical simulation of land subsidence above an off-shore Adriatic hydrocarbon reservoir, Italy, by Data Assimilation techniques 382: 449–55, https://doi.org/10.5194/piahs-382-449-2020.

Galloway, D. L., and T. J. Burbey. 2011. Regional land subsidence accompanying groundwater extraction. *Hydrogeology Journal* 19, no. 8: 1459.

Gambolati, G. 1975. Numerical models in land subsidence control. *Computer Methods in Applied Mechanics and Engineering* 5: 227–37.

Gambolati, G., and R. A. Freeze. 1973. Mathematical simulation of the subsidence of Venice: 1. Theory. *Water Resources Research* 9, no. 3: 721–33.

Gambolati, G., and P. Teatini. 2015. Geomechanics of subsurface water withdrawal and injection. *Water Resources Research* 51, no. 6: 3922–55.

Geospatial Information Authority of Japan. 2019. Technical Report of the Geospatial Information Authority of Japan, D1-No.957, Digital elevation topographic map of Niigata Prefecture.

Haider, A., G. Lee, T. H. Jafri, P. Yoon, J. Piao, and K. Jhang. 2023. Enhancing Accuracy of Groundwater Level Forecasting with Minimal Computational Complexity Using Temporal Convolutional Network. *Water* 15, no. 23: 4041.

He, K., X. Zhang, S. Ren, and J. Sun. 2016. Deep residual learning for image recognition. In *Proceedings of the IEEE conference on computer vision and pattern recognition*, 770–78.

Holzer, T. L., and D. L. Galloway. 2005. Impacts of land subsidence caused by withdrawal of underground fluids in the United States. *Reviews in Engineering Geology* 16: 87–99.

Japan Meteorological Agency. 2021. Climatological Normals of Takada, Niigata Prefecture, https://www.data.jma.go.jp/obd/stats/data/mdrr/normal/index.html.

Japan Meteorological Agency. 2024. Historical Weather Data Download, https://www.data.jma.go.jp/gmd/risk/obsdl/index.php.

Kayane, I. 1980. Groundwater use for snow melting on the road. *GeoJournal* 4: 173–81.

Kingma, D. P., and J. Ba. 2014. Adam: A method for stochastic optimization. *arXiv preprint arXiv:1412.6980*.

Lara-Benítez, P., M. Carranza-García, J. M. Luna-Romera, and J. C. Riquelme. 2020. Temporal convolutional networks applied to energy-related time series forecasting. *applied sciences* 10, no. 7: 2322.

Lea, C., M. D. Flynn, R. Vidal, A. Reiter, and G. D. Hager. 2017. Temporal convolutional networks for action segmentation and detection. In *proceedings of the IEEE Conference on Computer Vision and Pattern Recognition*, 156–65.

Liu, C.-Y., C.-Y. Ku, and J.-F. Hsu. 2023. Reconstructing missing time-varying land subsidence data using back propagation neural network with principal component analysis. *Scientific Reports* 13, no. 1: 17349.

Long, J., E. Shelhamer, and T. Darrell. 2015. Fully convolutional networks for semantic segmentation. In *Proceedings of the IEEE conference on computer vision and pattern recognition*, 3431–40.

Ma, T., Y. Du, R. Ma, C. Xiao, and Y. Liu. 2018. Water-rock interactions and related eco-environmental effects in typical land subsidence zones of China. *Hydrogeology Journal* 26, no. 5.

Mizumura, K. 1994. Prediction of land subsidence due to ground-water use in snow country. *Journal of Hydraulic Engineering* 120, no. 4: 448–60.

Modoni, G., G. Darini, R. L. Spacagna, M. Saroli, G. Russo, and P. Croce. 2013. Spatial analysis

of land subsidence induced by groundwater withdrawal. *Engineering Geology* 167: 59–71, https://doi.org/10.1016/j.enggeo.2013.10.014.

Morita, K., and M. Tago. 2005. Snow-melting on sidewalks with ground-coupled heat pumps in a heavy snowfall city. In *Proceedings of the World Geothermal Congress*.

Nair, V., and G. E. Hinton. 2010. Rectified linear units improve restricted boltzmann machines. In *Proceedings of the 27th international conference on machine learning (ICML-10)*, 807–14.

Ortega-Guerrero, A., D. L. Rudolph, and J. A. Cherry. 1999. Analysis of long-term land subsidence near Mexico City: Field investigations and predictive modeling. *Water resources research* 35, no. 11: 3327–41.

Pang, M., E. Du, C. A. Shoemaker, and C. Zheng. 2022. Efficient, parallelized global optimization of groundwater pumping in a regional aquifer with land subsidence constraints. *Journal of Environmental Management* 310: 114753.

Raskutti, G., M. J. Wainwright, and B. Yu. 2014. Early stopping and non-parametric regression: an optimal data-dependent stopping rule. *The Journal of Machine Learning Research* 15, no. 1: 335–66.

Remy, P. 2020. Temporal Convolutional Networks for Keras. *GitHub repository*. GitHub, https://github.com/philipperemy/keras-tcn.

Salimans, T., and D. P. Kingma. 2016. Weight normalization: A simple reparameterization to accelerate training of deep neural networks. *Advances in neural information processing systems* 29.

Sekiya, K., I. Tohno, N. Suzuki, N. Moriyama, and I. Tohno. 1997. Study on subsidence in every section in urban Tadaka, Joetsu, Niigata. *Research Report from the National Institute for Environmental Studies*, *Japan, No. 135*.

Sekiya, K., I. Tohno, and I. Tohno. 1997. Actual state of the land subsidence in the Takada Plain, Niigata, Japan. *Research Report from the National Institute for Environmental Studies*, *Japan, No. 135*.

Shirzaei, M., J. Freymueller, T. E. Törnqvist, D. L. Galloway, T. Dura, and P. S. Minderhoud. 2021. Measuring, modelling and projecting coastal land subsidence. *Nature Reviews Earth*

& Environment 2, no. 1: 40–58.

Smith, R., and R. Knight. 2019. Modeling Land Subsidence Using InSAR and Airborne Electromagnetic Data. *Water Resources Research* 55: 2801–19, https://doi.org/10.1029/2018WR024185.

Srivastava, N., G. Hinton, A. Krizhevsky, I. Sutskever, and R. Salakhutdinov. 2014. Dropout: a simple way to prevent neural networks from overfitting. *The journal of machine learning research* 15, no. 1: 1929–58.

Tohno, I., K. Sekiya, and I. Tohno. 1997. Subsurface geology based on boring observation at the urban Takada, Joetsu, Niigata, Japan. *Research Report from the National Institute for Environmental Studies*, *Japan, No. 135*.

Wan, R., S. Mei, J. Wang, M. Liu, and F. Yang. 2019. Multivariate temporal convolutional network: A deep neural networks approach for multivariate time series forecasting. *Electronics* 8, no. 8: 876.

Xu, Y.-S., S.-L. Shen, Z.-Y. Cai, and G.-Y. Zhou. 2008. The state of land subsidence and prediction approaches due to groundwater withdrawal in China. *Natural Hazards* 45: 123–35.

Yang, S., H. Lian, B. Xu, H. V. Thanh, W. Chen, H. Yin, and Z. Dai. 2023. Application of robust deep learning models to predict mine water inflow: Implication for groundwater environment management. *Science of the Total Environment* 871: 162056.

Yu, F., and V. Koltun. 2015. Multi-scale context aggregation by dilated convolutions. *arXiv preprint arXiv:1511.07122*.

Yuan, X., S. Qi, Y. Wang, K. Wang, C. Yang, and L. Ye. 2021. Quality variable prediction for nonlinear dynamic industrial processes based on temporal convolutional networks. *IEEE Sensors Journal* 21, no. 18: 20493–503.

Zhang, Xiaoying, F. Dong, G. Chen, and Z. Dai. 2023. Advance prediction of coastal groundwater levels with temporal convolutional and long short-term memory networks. *Hydrology and Earth System Sciences* 27, no. 1: 83–96.

Zhang, Xuan, and D. Li. 2023. Multi-input multi-output temporal convolutional network for

predicting the long-term water quality of ocean ranches. *Environmental Science and Pollution Research* 30, no. 3: 7914–29.

Zhang, Y., Y. Xue, J. Wu, H. Wang, and J. He. 2012. Mechanical modeling of aquifer sands under long-term groundwater withdrawal. *Engineering Geology* 125: 74–80.

Zhang, Y., Y. Xue, J. Wu, and Z. Wang. 2015. Compaction of aquifer units under complex patterns of changing groundwater level. *Environmental Earth Sciences* 73: 1537–44.